Article

Efficient Epoxidation of a Terminal Alkene Containing Allylic Hydrogen Atoms: *trans*-Methylstyrene on Cu{111}

Rachael L. Cropley, Federico J. Williams, Andrew J. Urquhart, Owain P. H. Vaughan, Mintcho S. Tikhov, and Richard M. Lambert

J. Am. Chem. Soc., **2005**, 127 (16), 6069-6076• DOI: 10.1021/ja042758e • Publication Date (Web): 05 April 2005

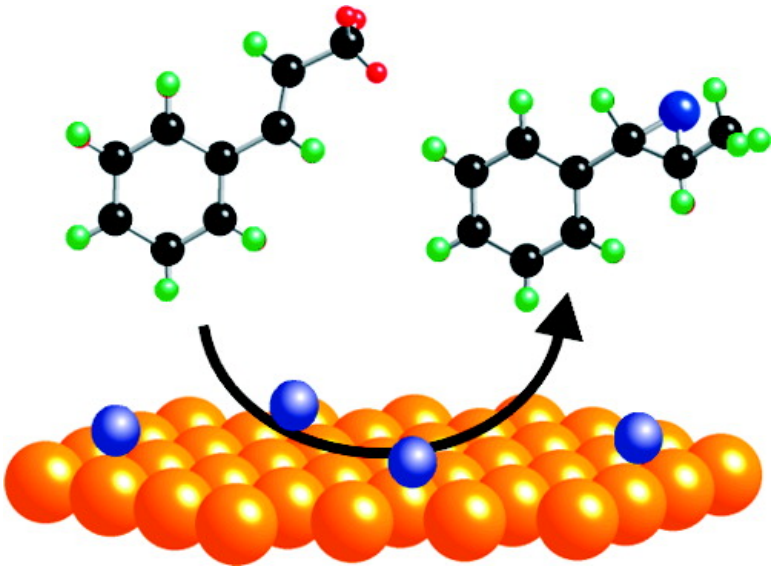

J|A|C|S
ARTICLES
Published on Web 04/05/2005

Efficient Epoxidation of a Terminal Alkene Containing Allylic Hydrogen Atoms: *trans*-Methylstyrene on Cu{111}

Rachael L. Cropley, Federico J. Williams, Andrew J. Urquhart, Owain P. H. Vaughan, Mintcho S. Tikhov, and Richard M. Lambert*

Contribution from the Department of Chemistry, University of Cambridge, Cambridge, CB2 1EW, UK

Received December 1, 2004; E-mail: RML1@cam.ac.uk

Abstract: The selective oxidation of *trans*-methylstyrene, a phenyl-substituted propene that contains labile allylic hydrogen atoms, has been studied on Cu{111}. Mass spectrometry and synchrotron fast XPS were used to detect, respectively, desorbing gaseous products and the evolution of surface species as a function of temperature and time. Efficient partial oxidation occurs yielding principally the epoxide, and the behavior of the system is sensitive to the order in which reactants are adsorbed. The latter is understandable in terms of differences in the spatial distribution of oxygen adatoms; isolated adatoms lead to epoxidation, while islands of "oxidic" oxygen do not. NEXAFS data taken over a range of coverages and in the presence and absence of coadsorbed oxygen indicate that the adsorbed alkene lies essentially flat with the allylic hydrogen atoms close to the surface. The photoemission results and comparison with the corresponding behavior of styrene on Cu{111} strongly suggest that allylic hydrogen abstraction is indeed a critical factor that limits epoxidation selectivity. An overall mechanism consistent with the structural and reactive properties is proposed.

Introduction

Even though it provides the basis for a mature large-scale technology, the silver-catalyzed heterogeneous epoxidation of ethene remains a subject of enduring interest to both experimentalists and theorists, mainly due to continuing debate over some aspects of the reaction mechanism. Nevertheless, there is broad consensus about the nature of the key surface species involved.[1]

In contrast, the heterogeneous epoxidation of higher terminal alkenes that contain labile allylic H atoms is much more challenging and also technologically highly desirable. This subject has been far less investigated, despite the fact that propene epoxide, for example, is a far more valuable chemical intermediate than ethene epoxide. Thus Ag is a very inefficient catalyst for the epoxidation of propene, delivering selectivities of the order of ~5%[2] which is to be compared with ~80% selectivity routinely achieved in the case of ethene epoxidation under similar conditions. The inefficiency of Ag toward propene epoxidation is often ascribed[3] to the facile loss of a hydrogen atom by the sp^3 carbon resulting in stable, strongly adsorbed allylic species whose ultimate fate can only be combustion. Though plausible, this important hypothesis has yet to be established.

In passing, we note that high propene epoxide selectivities, albeit at low reactant conversion, may be achieved with Au/TiO_2 catalysts of the type pioneered by Haruta et al.[4,5] However, these systems depend critically on the presence of large amounts of co-fed hydrogen, most of which ends up as water. The corresponding reaction mechanism remains obscure, though we may conclude that the chemistry must be distinct from that which operates when, as here, no gaseous hydrogen is present.

The reactivity toward oxygen of ethene on well-defined single-crystal surfaces of silver cannot be studied under ultrahigh vacuum (UHV) conditions due to the associated low adsorption enthalpy; the alkene desorbs before it can react. On the other hand styrene (phenylethene) is much more strongly adsorbed, and its use as a model molecule in substitution for ethene provides a means of investigating the oxidative chemistry of such nonallylic alkenes when adsorbed on silver: this strategy has proved successful in elucidating key mechanistic aspects of epoxidation on Ag single-crystal surfaces.[6,7]

By means of similar experiments on Cu{110}[8] and Cu{111},[9] we were able to demonstrate that not only is Cu effective in inducing the epoxidation of styrene and butadiene but also it is actually far more selective than Ag,[10] delivering selectivities close to 100% under UHV conditions. *Why* copper appears to be intrinsically better than silver is a question that can be

(1) Van Santen, R. A.; Kuipers, H. P. C. E. *Adv. Catal.* **1998**, *35*, 265.
(2) Akimoto, M.; Ichikawa, K.; Echigoya, E. *J. Catal.* **1982**, *76*, 333.
(3) Ossipoff, N. J.; Cant, N. W. *Catal. Lett.* **1992**, *16*, 149.
(4) Hayashi, T.; Tanaka, K.; Haruta, M. *J. Catal.* **1998**, *178*, 566.
(5) Haruta, M.; Yamada, N.; Kobayashi, T.; Iijima, S. *J. Catal.* **1989**, *115*, 301.
(6) Hawker, S.; Mukoid, C.; Badyal, J. P. S.; Lambert, R. M. *Surf. Sci.* **1989**, *219*, L615.
(7) Williams, F. J.; Bird, D. P. C.; Palermo, A.; Santra, A. K.; Lambert, R. M. *J. Am. Chem. Soc.* **2004**, *126*, 8509.
(8) Cowell, J. J.; Santra, A. K.; Lindsay, R.; Lambert, R. M.; Baraldi, A.; Goldoni, A. *Surf. Sci.* **1999**, *437*, 1.
(9) Santra, A. K.; Cowell, J. J.; Lambert, R. M. *Catal. Lett.* **2000**, *67*, 87.
(10) Roberts, J. T.; Capote, A. J.; Madix, R. J. *J. Am. Chem. Soc.* **1991**, *113*, 9848.

addressed by means of theory. DFT calculations[11] show that one fundamental factor is the inversion in the ordering activation barriers for epoxidation versus combustion in going from Ag to Cu: epoxidation is less activated than combustion on Cu and the opposite is true for Ag. Our aim here is a mechanistic study of the oxidation chemistry of a propene analogue on a metal surface that is likely to be more selective than Ag. Accordingly we have investigated the adsorption geometry and oxidation chemistry of the propene-mimic *trans*-methylstyrene (TMS) on Cu{111} (propene itself desorbs from Cu{111} at only ~130 K[12]). Propene adsorbs on Cu{111} with the C═C bond almost parallel to the metal surface;[13] as we shall show, the same is true for the C═C bond in TMS, thus validating the use of this molecule as a propene-mimic. We find that TMS exhibits marked selective oxidation activity on Cu{111}, the principal carbon-containing gaseous product being *trans*-methylstyrene epoxide.

Experimental Methods

Temperature programmed reaction (TPR) experiments were performed in Cambridge using a UHV chamber of conventional design; this apparatus and the methods used for sample mounting and manipulation are described elsewhere.[14] Before each experiment the Cu{111} sample was cleaned by Ar^+ sputtering and annealed to 800 K, surface quality being checked by Auger and LEED. TMS and oxygen were dosed by backfilling the chamber; doses are quoted in Langmuirs ($1\ L = 1 \times 10^{-6}$ Torr s^{-1}), uncorrected for differences in ionization cross sections. TPR spectra were acquired with a heating rate of 8 K s^{-1}, with the ionizer of the quadrupole mass spectrometer located ~1 cm from the crystal front face. Our quadrupole mass spectral fragmentation patterns were normalized to permit comparison with NIST standard spectra by quantitative evaluation of the mass discrimination effects inherent in quadrupole mass filters. This was done by measuring the parent ion intensities of a range of molecules (CO, Ar, TMS, Xe; *m*/*z* 20−131) at known total pressures (corrected for ionization gauge sensitivity) so as to produce a calibration curve of *m*/*z* versus the required correction factor.

Fast XPS and C K-edge NEXAFS measurements were carried out on the SuperESCA beamline at the ELETTRA synchrotron radiation source in Trieste, Italy. The degree of linear polarization of the photons was 0.99, and the photon energy was calibrated (±0.2 eV) by the position of C K-edge dip in the monochromator output. XPS and NEXAFS spectra were collected using a double pass 32-channel hemispherical electron analyzer. The angle between the entrance lens of the analyzer and the incoming photon beam was 70° in the horizontal plane. Methods employed for sampling cleaning and gas dosing were the same as those used in Cambridge. Fast XPS experiments were performed at a heating rate of 0.5 K s^{-1} using photon incidence and photoelectron detection angles of 8° and 78°, respectively, relative to the surface. No beam-induced decomposition of the adsorbed layer was observed during these experiments. The XPS data acquisition rate was ~20 s/spectrum for C 1s and ~30 s/spectrum for O 1s, corresponding to temperature increments between scans of 10 and 15 K, respectively. As the heating rate used for the fast XPS experiments was ~16 times lower than that used for the (Cambridge) TPR experiments, desorption peak temperatures in the former case are expected to be ~20 K lower than those in the latter case. All spectra are referenced to the Cu $3p_{3/2}$ line. Coverages in the synchrotron experiments were calculated by reference to XP spectral intensities monitored during continuous adsorption of TMS ($T = 200$ K). The 0.5 eV shift in binding energy that occurred upon completion of the first adsorbed layer was readily identifiable: this point corresponds to 2.6×10^{14} TMS molecules cm^{-2}. Corresponding measurements were not possible in the laboratory studies so that TPR results are presented in terms of exposures rather than coverages. Since the sizes of O_a and TMS are very different, their monolayer saturation coverages are also very different: a full monolayer of oxygen would contain about three times as many atoms as the number of TMS molecules in a full monolayer. To avoid confusion, oxygen and TMS fractional coverages (Θ) are therefore specified with respect to the number density of Cu atoms in the {111} surface, and thus Θ_X = number density of X/1.77×10^{15} cm^{-2}. The estimated error in quoted coverages is ±10%.

Results

As we shall see, the adsorption sequence (TMS first, then oxygen, or vice versa) had a pronounced effect on the subsequent behavior; the differences highlight particular aspects of the reaction mechanism.

Temperature Programmed Reaction: TMS First, Then Oxygen. Figure 1a−e show TPR spectra obtained after dosing the surface first with 1 L of TMS at 170 K followed by a range of O_2 doses, also administered at 170 K. TMS adsorbed and desorbed reversibly from the clean surface yielding a peak at 245 K (Figure 1a, bottom spectrum): in this case, neither carbon deposition nor desorption of any other species was detected. (In passing, we note that TMS always formed disordered overlayers (LEED).) The presence of O_a upshifted the m/z = 117 TMS peak (α) by ~50 K relative to the clean surface case; in addition, a 360 K peak (β) ascribed to a more tightly bound form of TMS became prominent at high oxygen exposures. The nature of this β species is explored in more detail later, under conditions where its relative concentration was higher. The onset of TMS combustion at higher oxygen coverages is signaled by the evolution of water (Figure 1d) and carbon dioxide (Figure 1e); notice that CO_2 production exhibits a distinct threshold between 50 and 100 L and that this correlates with the onset of the β TMS species. We may conclude that H_2O and CO_2 are formed by surface reaction rate-limited processes, because adsorbed water and CO_2 desorb from Cu{111} at temperatures below 170 K.[15,16]

The m/z = 90, 105 spectra provide a clear indication of the formation of substantial amounts of partial oxidation product(s). Very small coincident signals at *m*/*z* 134 were also detected but were too noisy to be of quantitative use; they correspond to the parent ion of TMS epoxide and the isomeric ketones. Clearly, the oxygenated copper surface induces selective oxidation of TMS rather effectively, despite the presence of allylic hydrogen atoms. These spectra are therefore of considerable interest.

Trans-methylstyrene epoxide, benzylmethyl ketone, and 1-phenyl,1-propanone are in principle distinguishable by the relative intensities of their fragment ion peaks at m/z = 90 and 105 (both ketones are possible isomerization products of an initially formed epoxide) which, respectively, are as follows: 90:105 = 1:0.6, 1:0.24, and 0:0.1.[17] Therefore 1-phenyl,1-propanone may be excluded because it gives no signal at m/z = 90. Given the fragmentation pattern of TMS,[17] the m/z =

(11) Torres, D.; Illas, F.; Lopez, N.; Lambert, R. M. *J. Am. Chem. Soc.*, submitted.
(12) Meyers, J. M.; Gellman, A. J. *Surf. Sci.* **1995**, *339*, 57.
(13) Street, S. C.; Gellman, A. J. *J. Phys. Chem. B* **1997**, *101*, 1389.
(14) Middleton, R. L.; Lambert, R. M. *Catal. Lett.* **1999**, *59*, 15.
(15) Hadenfeldt, S.; Benndorf, C.; Stricker, A.; Towe, M. *Surf. Sci.* **1996**, *352*, 295.
(16) Hinch, B. J.; Dubois, L. H. *J. Chem. Phys.* **1992**, *96* (4), 3262.
(17) NIST Chemistry Webbook, http://webbook.nist.gov/.

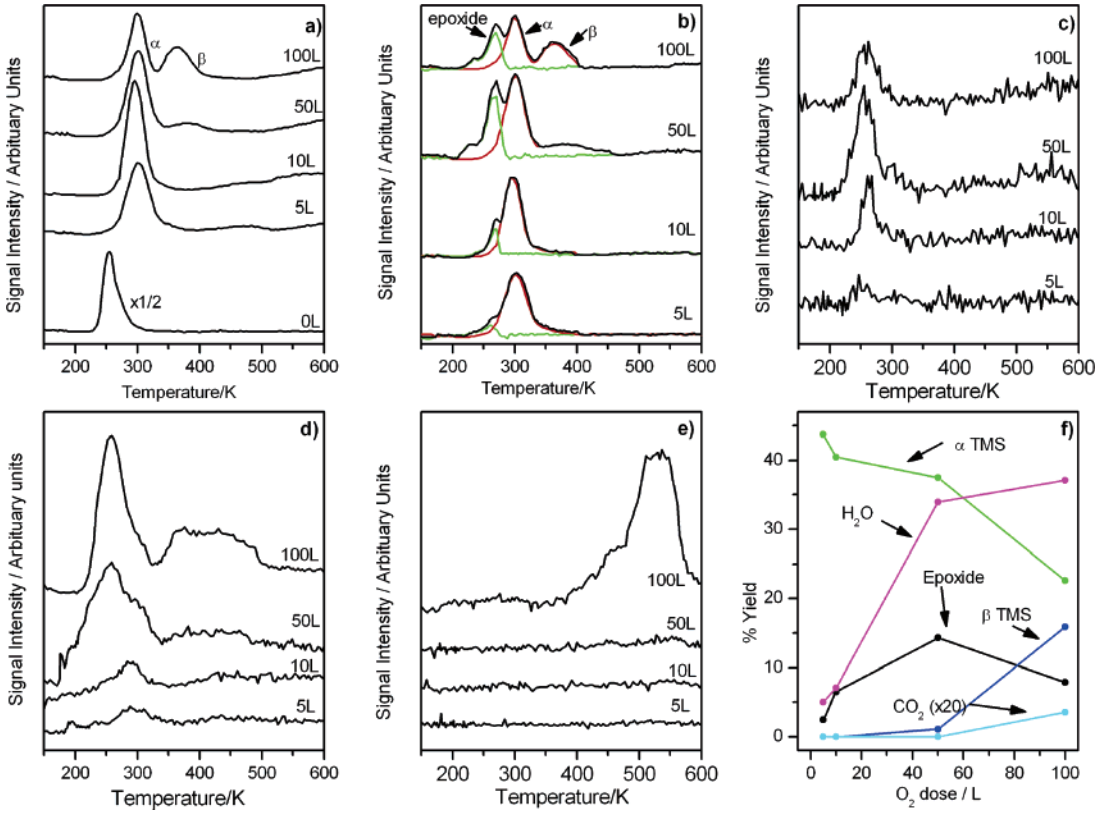

Figure 1. TPR spectra showing products from the reaction between preadsorbed TMS (1 L) and varying amounts of subsequently adsorbed oxygen (5−100 L). (a) $m/z = 117$, (b) $m/z = 90$, (c) $m/z = 105$, (d) $m/z = 18$, (e) $m/z = 44$, (f) integrated yields of products (see text).

117 spectra may be used to calculate the contribution of TMS to the $m/z = 90$ spectra, shown as the red curves. Subtraction of these from the raw data yields residuals (green curves) whose integrated intensities correspond to 90:105 relative intensities of 1:0.4 ± 0.2. Within the experimental error, this ratio does not permit us to distinguish between TMS epoxide and benzylmethyl ketone. However, although the intensity *ratio* of these fragment ions is similar for the two molecules, their *absolute* intensities are very different; in fact the ionization yield of $m/z = 90$ is 50 times smaller for benzylmethyl ketone compared to TMS epoxide. Thus if benzylmethyl ketone were the principal product, our data would imply that the amount of benzylmethyl ketone produced was ∼5 times greater than the amount of TMS initially present on the surface, clearly not possible. Therefore, on grounds of mass balance, the implication is that TMS epoxide is the principal product, *although we cannot rule out the formation of small amounts of the ketone.* In passing, we note that in the case of styrene epoxidation on Ag(111)[6] and Ag(100),[7] no acetophenone was formed. Moreover in the case of styrene oxidation on TiO_2,[18] it was found that when the epoxide and the ketone desorbed from the surface they were readily distinguishable. The small shoulder at ∼230 K in the epoxide spectra which is apparent only at the highest oxygen coverages deserves comment (Figure 1b). Its presence suggests that higher oxygen coverages induce a somewhat lower temperature pathway for the formation of gaseous epoxide, although we are unable to speculate further as to the origin of this effect.

Figure 1f summarizes the TPR results in terms of integrated desorption yields of the various species. Note that production of epoxide goes through a maximum at an oxygen exposure of 50 L at which point β TMS and CO_2 formation commences. In this figure, the term "% yield" refers to the percentage of the initially adsorbed TMS that desorbs as each of the various species. The necessary quantitative calibration was obtained by considering the TPR results alongside the C 1s XPS data (Figure 3b, see later). Thus stage 1 in Figure 3b is due to desorption of αTMS and epoxide, the ratio of TMS, and epoxide yields being known from the respective TPR integrated intensities at the corresponding coverage, normalized as described in the experimental methods section. Stage 2 in Figure 3b is due to desorption of βTMS, and of course the residual C 1s intensity is a measure of what remains on the surface. Because of the difficulty of directly calibrating the mass spectrometer for sensitivity toward H_2O, this quantity was determined indirectly using the corresponding O 1s XPS data (see later). In terms of carbon-containing *gaseous* products, it is clear that the system is very selective toward epoxide formation. Thus, for a 50 L O_2 dose (corresponding to an oxygen fractional surface coverage, Θ_O, of ∼0.07) effectively *all* the TMS that yields carbon-containing gaseous products ends up as epoxide; ∼45% of the originally adsorbed TMS is retained on the surface as carbonaceous residue.

Temperature Programmed Reaction: Oxygen First, Then TMS. As will become apparent, this adsorption sequence gave rise to some notable differences in behavior compared to the opposite sequence, which it is useful to summarize here.

1. The onset of β TMS formation occurred at significantly lower oxygen exposures.

2. The second H_2O peak was much more pronounced.

(18) Sykes, E. C. H.; Tikhov, M. S.; Lambert, R. M. *Catal. Lett.* **2002**, *78*, 7.

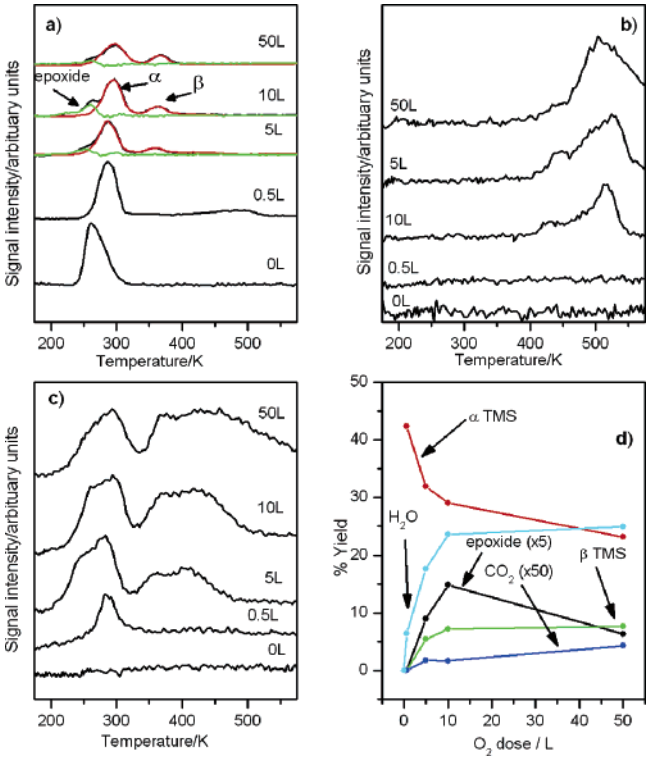

Figure 2. TPR spectra showing products from the reaction between preadsorbed O_2 and TMS (1 L) on Cu{111}for various O_2 doses (a) m/z = 90, (b) m/z = 44, (c) m/z = 18, (d) integrated yields of products.

3. Two rather than three oxygen species were detected in XPS (see later).

Figure 2 shows the effects of reversing the exposure sequence, 1 L of TMS, as before, but this time *preceded* by varying doses of oxygen. As we shall see, this results in several differences in behavior. Only the m/z = 90, 44, 18 spectra are shown, as these bring significant new information. It is apparent that the onset of appreciable water and CO_2 production occurs at much lower oxygen exposures than under the opposite dosing sequence, that the second H_2O peak is relatively much more pronounced than previously (Figure 2b, c), and that for a given oxygen dose the β: α TMS ratio is *much* higher than before (Figure 2a; 1:3 compared to 1:36 for a 50 L oxygen dose). Notice also that the overall conversion to selective oxidation products is less than that with the opposite dosing sequence. Aided by the fast XPS data to be presented below, we shall argue that these effects of altering the reactant dosing sequence are understandable in terms of differences in the spatial distribution of adsorbed oxygen.

Temperature Programmed XPS: TMS First, Then Oxygen. As we shall see, the TPR and C 1s fast XPS results agree well in regard to both the desorption temperatures (taking into account the differences in heating rates) and the yields of the various gaseous products. Figure 3a shows temperature programmed C 1s fast-XP spectra acquired during reaction after first dosing the surface at 200 K with Θ_{TMS} of 0.07 followed by Θ_o of 0.07. In principle, at least four different carbon-containing species are to be expected: the α and the β forms of TMS, the epoxide, and carbonaceous fragments. No CO_2 should have been detectable as the TPR results show that this product desorbs immediately upon formation. By comparison with the corresponding TPR results (Figure 1, 50 L dose), the

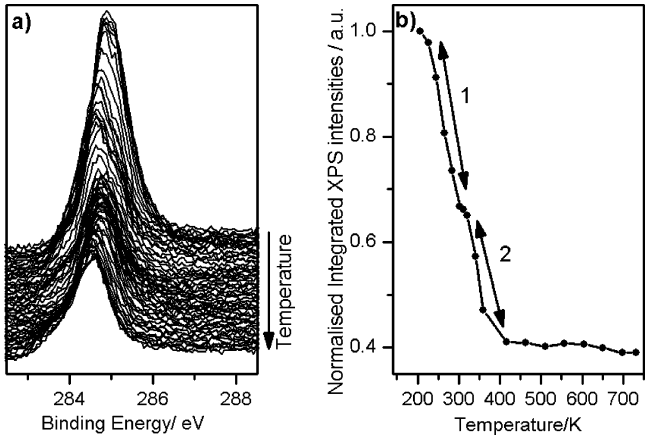

Figure 3. C 1s fast XP spectra showing the reaction products from preadsorbed TMS (Θ_{TMS} = 0.07) followed by Θ_o = 0.07 of oxygen: (a) C 1s XP spectra, (b) C1s total integrated intensity (note origin of y axis).

raw data in Figure 3a correspond to the presence of α and β TMS and carbonaceous fragments. These components cannot be resolved with confidence. Therefore only the variation of the total integrated intensity is shown in Figure 3b. In region 1, between 255 and 300 K, the C 1s intensity decreases and the peak shifts from 284.9 to 284.7 eV. Comparison with TPR data (Figure 1, 50 L of O_2), taking into account the different heating rates, indicates that this corresponds to desorption of α TMS and the epoxide. Correspondingly, in region 2 (325 K−385 K) the next stage of carbon loss corresponds to β TMS desorption. With increasing temperature, as further decomposition of the carbonaceous residue occurs, the C 1s peak shifts gradually to lower binding energy accompanied by a slight decrease in the amount of surface carbon as a very small amount of CO_2 desorbs from the surface. These results show that, under the conditions employed, 10% of the initially adsorbed TMS formed epoxide, 25% of both the α and β TMS desorbed without reaction, and an amount of carbonaceous residue equivalent to 40% of the initial TMS remained on the surface. (This agrees well with the TMS desorption yields calculated from the TPR data in Figure 1.)

Figure 4a shows the corresponding O 1s fast XPS spectra, and the derived integrated intensities are shown in Figure 4b. In this case, three oxygen species are clearly discernible: (1) adsorbed OH at 531.2 eV,[19,20] (2) "ordinary" O_a[21] and oxidic oxygen[22] at 529.6 eV and (3) an unusual species at 528.9 eV that we designate as metastable atomic oxygen,[21] O* (the peak at ∼537 eV is a Cu Auger transition).

All three peaks were fitted with Gaussians with fwhms of 1.4 eV. Note that abundant OH is present from the very start, at 200 K, presumably the result of H abstraction from TMS. Its concentration declined steeply between 230 and 280 K which, according to the TPR results, corresponds to the first stage of water evolution. At the same time the metastable O* species underwent conversion to O_a. The concentration of the latter maximized at ∼300 K, which corresponds to the onset of the

(19) http://srdata.nist.gov/xps/ NIST X-ray Photoelectron Spectroscopy Database NIST Standard Reference Database 20, Version 3.4 (Web Version).
(20) Ammon, Ch.; Bayer, A.; Steinrück, H.-P.; Held, G. *Chem. Phys. Lett.* **2003**, *377*, 163.
(21) Davies, P. R.; Roberts, M. W.; Shukla, N.; Vincent, D. J. *Surf. Sci.* **1995**, *325*, 50.
(22) Carley, A. F.; Davies, P. R.; Roberts, M. W.; Vincent, D. J. *Top. Catal.* **1994**, *1*, 35.

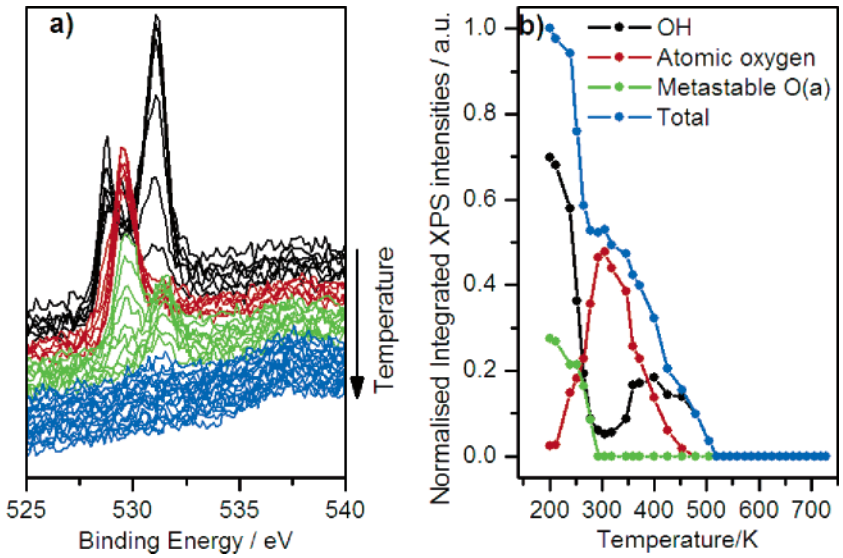

Figure 4. O 1s fast XP spectra showing reaction products from preadsorbed TMS ($\Theta_{TMS} = 0.07$) dosed with Θ_O of 0.07: (a) O 1s XP spectra (different colors used to clarify evolution of spectra), (b) integrated intensities.

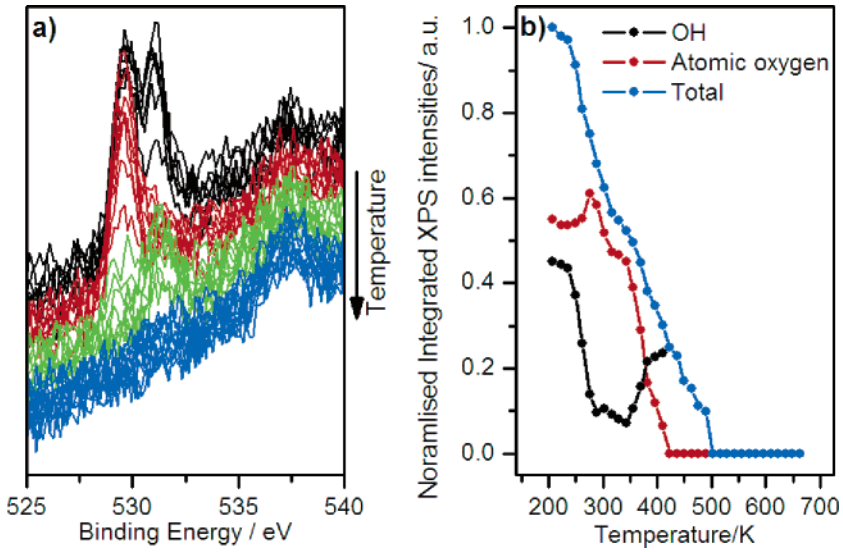

Figure 5. O 1s fast XPS spectra showing the reaction products from $\Theta_o = 0.04$ of predosed oxygen followed by TMS ($\Theta_{TMS} = 0.04$). (a) O 1s XP spectra (different colors used to clarify evolution of spectra), (b) O 1s integrated intensities.

second stage of water production; it then declined, eventually vanishing at ~450 K, which corresponds to the final stages of water evolution in the TPR spectra. Notice also the pronounced minimum in OH concentration at ~310 K, followed by a maximum at ~415 K, to be discussed later.

Temperature Programmed XPS: Oxygen First, Then TMS. Figure 5a shows O 1s fast-XP data acquired after using the reverse dosing sequence at 200 K: preadsorption of $\Theta_o = 0.04$ ML of oxygen followed by TMS ($\Theta_{TMS} = 0.04$). Figure 5b shows the integrated intensities derived from the raw data. The corresponding C 1s fast XPS results are similar to those presented in Figure 3 and are therefore not shown here. (Adsorbate coverages required for optimum reactivity differed from those used for Figure 4, presumably reflecting the different spatial distribution of reactants in the two cases, as argued below.)

In contrast with the results presented immediately above, here only *two* oxygen peaks appeared: OH centered at 531.2 eV and O_a and oxidic oxygen at 529.6 eV. The metastable oxygen species (O*) found above (528.9 eV) was not detected. *Moreover O_a was detectable from the very start, whereas previously it was not* (see Figure 4). OH species, most likely originating from the immediate abstraction of allylic hydrogens, were present from the beginning, as before; the variation in their concentration was also similar to that found previously (Figure 4b). Notice the distinct maximum at 275 K in the O_a intensity and the fact that all surface oxygen had been consumed by the end of the experiment, as before (Figure 4b).

NEXAFS of Adsorbed TMS as a Function of Coverage and in the Absence and Presence of O_a. Figure 6 shows C K-edge step normalized NEXAFS data, recorded at grazing and normal photon incidence angles as a function of TMS coverage and also after coadsorption of $\Theta_o = 0.04$ of oxygen and $\Theta_{TMS} = 0.04$ of TMS (the same conditions as for Figure 2, 10 L dose, and Figure 5). Normalization followed an established procedure[23] with the edge jump set to the XPS binding energy plus

(23) Outka, D. A.; Stohr, J. *J. Chem. Phys.* **1988**, *88*, 3539.

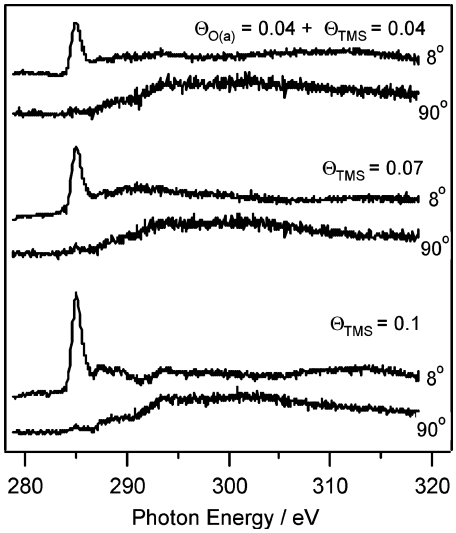

Figure 6. Carbon K-edge NEXAFS spectra acquired at normal and grazing incidence for $\Theta_{TMS} = 0.07$ of TMS, $\Theta_{TMS} = 0.10$ of TMS, and ($\Theta_o = 0.04$ of oxygen + $\Theta_{TMS} = 0.04$ of TMS) all at 180 K.

the work function of the clean surface (4.94 eV).[24] The dominant feature is a sharp peak at ~285 eV, which, by comparison with C *K*-edge NEXAFS for benzene and ethene,[25−28] may be assigned to a transition from C 1s to a π^* orbital. The comparison with benzene and ethene is relevant as TMS contains both a phenyl and a vinyl group. In the case of styrene, these two components are resolved in the NEXAFS, the vinyl and phenyl group resonances occurring at 284.3 and 285 eV,[29] respectively. In the present case, the two components are not resolved. Detailed calculations are necessary in order to analyze this resonance fully so as to detect distortions from coplanarity; these are in progress.[30]

It is evident from inspection of the data that the π^* resonance intensity is highest at the grazing photon incidence angle and decreases as the angle is increased, almost vanishing at normal incidence; the σ^* resonances exhibit the opposite behavior. Thus TMS is adsorbed such that phenyl and vinyl groups are essentially parallel to the Cu surface.

A more detailed analysis of the π^* intensity variation following standard procedures described by Stohr[27] permits a quantitative estimate of the molecular tilt angle (α). The results of this procedure yield an apparent tilt angle of TMS is ~10° ± 5, independent of coverage and regardless of the presence of oxygen. Therefore it is reasonable to interpret all the reactive behavior of TMS in terms of just one adsorption geometry.

Discussion

The differences in reactive behavior resulting from reversing the dosing order of TMS and O_2 may be rationalized in terms of the adsorption properties of oxygen on Cu{111}. STM studies[31] show that at exposures > 100 L, dissociative chemisorption of oxygen on Cu{111} leads eventually to nucleation and growth of 2D triangular islands of Cu_2O{111}. As will become apparent, the present results include several manifestations of this behavior which was most pronounced when oxygen was predosed, under which conditions it might be expected that oxidic island growth would be unchecked by any effects due to coadsorbed TMS.

The oxygen-induced 50 K upshift in the TMS desorption peak (Figure 1a) points to a strong interaction between O_a and the adsorbed alkene, and at sufficiently high oxygen coverages a distinctly different state of adsorbed TMS appears (β). We assign this β TMS to molecules associated with surface oxide islands, which in this case (preadsorbed TMS) nucleate and grow at O_2 exposures greater than 50 L.

The single most striking observation is the formation of TMS epoxide *even though allylic hydrogen atoms are present* in the starting alkene and they are close to the oxygenated surface. This stands in complete contrast to the behavior of TMS on single-crystal surfaces of Ag[32] where, under comparable conditions, combustion and carbon deposition are the only outcomes. Thus the intrinsic superiority of Cu over Ag in selective oxygen transfer is demonstrated again. Indeed, when we consider the series styrene,[8,7] butadiene,[10,33] and TMS, this superiority becomes more pronounced the more "difficult" the alkene.

The epoxide yield passes through a maximum at 50 L (Figure 1) beyond which point the amount of β TMS, and by inference the amount of oxygen in oxidic islands, increases substantially. The implication is that whereas isolated O_a is an effective epoxidizing agent, oxidic oxygen is a poor electrophile and therefore ineffective for partial oxidation.

Interestingly, although water production commences from the lowest oxygen coverages, it becomes appreciable only at ≥50 L and by 100 L two distinct stages are apparent. It seems plausible to suggest that the low-temperature peak is associated with H-abstraction due to O_a, while the broad high-temperature feature is due to reaction with oxidic oxygen; recall that the XPS results show that, by the end of the temperature sweep, all forms of oxygen have been consumed.

Figure 1a also shows that oxygen causes extensive decomposition of TMS to form hydrocarbonaceous residues (compare yields of TMS from clean and oxygen covered surfaces). Under steady-state catalytic conditions, such residues would presumably burn off to produce CO_2, so that their formation in these experiments is not likely to be of significance with respect to potential practical applications. Here, a small amount of high-temperature CO_2 production is only found at the highest oxygen coverage: under all conditions essentially all the surface oxygen is consumed to make water and partial oxidation products. The corresponding behavior of styrene on Cu{111} is very different: epoxidation is 100% selective with no cracking of the molecule to form carbonaceous deposits.[9] Therefore by comparison of the two cases, it is reasonable to conclude that with TMS it is indeed the presence of allylic hydrogen atoms at the additional sp^3 carbon atom that is critically important in determining

(24) Skriver, H. L.; Rosengaard, N. M. *Phys. Rev. B* **1992**, *46*, 7157.
(25) Horsley, J. A.; Stohr, J.; Hitchcock, A. P.; Newbury, D. C.; Johnson, A. L.; Sette, F. *J. Chem. Phys.* **1985**, *83*, 6099.
(26) Xi, M.; Yang, M. X.; Jo, S. K.; Bent, B. E.; Stevens, P. *J. Chem. Phys.* **1994**, *101*, 9122.
(27) Stohr, J.; Outka, D. A. *Phys. Rev. B* **1987**, *36*, 7891.
(28) Lee, A. F.; Wilson, K.; Lambert, R. M.; Goldoni, A.; Baraldi, A.; Paolucci, G. *J. Phys. Chem. B* **2000**, *104*, 11729.
(29) Williams, F. J.; Bird, D. P. C.; Sykes, E. C. H.; Santra, A. K.; Lambert, R. M. *J. Phys. Chem. B* **2003**, *107*, 3824.
(30) Kolczew, C.; Hermann, K.; Cropley, R. L.; Williams, F. J.; Vaughan, O. P. R.; Urquhart, A.; Lambert, R. M. In preparation.
(31) Matsumoto, T.; Bennett, R. A.; Stone, P.; Yamada, T.; Domen, K.; Bowker, M. *Surf. Sci.* **2001**, *471*, 225.
(32) Cropley, R. L.; Williams, F. J.; Vaughan, O. P. H.; Urquhart, A. J.; Tikhov, M. S.; Lambert, R. M. *Surf. Sci.* **2005**, *578*, L85.
(33) Cowell, J. J.; Santra, A. K.; Lambert, R. M. *J. Am. Chem. Soc.* **2000**, *122*, 2381.

epoxidation selectivity. Abstraction of one of these H atoms by oxygen precludes epoxidation because it results in a strongly adsorbed entity whose ultimate fate can only be combustion.

Reversing the adsorption sequence (oxygen first, then TMS) resulted in the appearance of β TMS at 5 L of O_2 exposure (as opposed to 50 L, previously) and lower selectivity toward epoxide formation (Figure 2). Both observations are consistent with the hypothesis that when oxygen is preadsorbed, oxidic island growth proceeds unchecked on the initially bare surface, whereas when TMS is preadsorbed, the oxygen has to be accommodated within the interstices of the TMS overlayer, thus inhibiting growth of oxidic islands. The H_2O results show that the high temperature peak is relatively much more pronounced than before (Figure 1), supporting the proposition advanced earlier that water formations is due to oxidation by oxidic oxygen. (In principle, 2D islands of Cu_2O could be detected by observing the shift in the Cu L_3VV Auger transition; however this was not possible in the presence of intense emission from the large amount of Cu^0.)

The O 1s fast XPS results combined with the corresponding TPR data provide additional insights into the overall mechanism (Figures 4 and 1). At 200 K, preadsorption of TMS followed by oxygen leads immediately to the formation of two oxygen species: OH and O*. One may speculate that the ease of formation at low temperature of this initially generated hydroxyl points to it having been produced by the stripping of allylic hydrogen. These subsequently desorb to yield water + O_a as clearly demonstrated by the decrease in OH in Figure 4 and the desorption of water at 280 K in Figure 1. The processes by which this occurs can be more clearly identified when considering the reverse dosing sequence, as discussed below. We assign O* to a metastable state of oxygen induced by the presence of preadsorbed TMS which forces the oxygen adatoms to occupy abnormal surface sites. A very similar effect has been reported in the case of ammonia coadsorption with oxygen on Cu{111}[21] where an O* species is formed and undergoes subsequent conversion to O_a with increasing temperature and decreasing surface coverage. The O 1s binding energies in the two cases are very similar (528.9 eV, here; 528.8 eV[34]). A second peak in the surface concentration of hydroxyl groups occurs at 315 K when the oxidic oxygen abstracts hydrogen atoms from hydrocarbonaceous residue to form hydroxyl groups.

Reversing the dosing sequence (O_2 first, then TMS) produced notably different O 1s spectra (Figure 5). Most strikingly, O* was completely absent. Again, this is consistent with all the other effects we have ascribed to the consequences of changing the order of adsorption. Preadsorbing oxygen allows unconstrained uptake of O_a with eventual nucleation and growth of 2D oxide; no oxygen is forced to occupy abnormal sites. The initial decrease in OH corresponds well with the low-temperature water peak in Figure 2b and the maximum in O_a concentration (Figure 5) indicating that the following process occurs: OH + OH $\rightarrow$ H_2O + O_a. If no other processes occurred, then the increase in O_a should be half the decrease in OH groups. As this is not the case, OH groups must also abstract additional hydrogen atoms from adsorbed organic species and then desorb as water. As suggested above, the second OH peak results from hydrogen abstraction induced by the oxidic oxygen.

(34) Davies, P. R.; Shukla, N.; Vincent, D. J. *J. Chem. Soc., Faraday Trans.* **1995**, *91*, 2885.

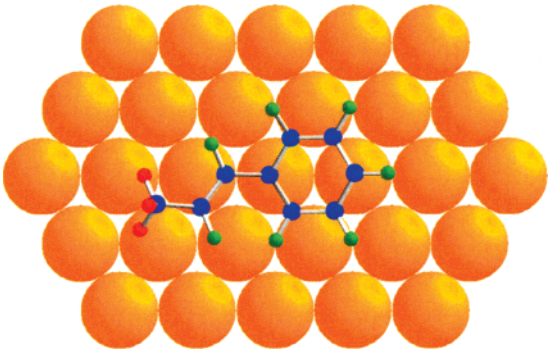

Figure 7. Flat-lying TMS, allylic hydrogen atoms shown in red.

The NEXAFS results indicate that *changes* in adsorption geometry of TMS as a function of coverage and oxygen coadsorption are not of significance. However, the actual adsorption geometry (essentially flat-lying, Figure 7) is interesting and relevant. In the gaseous[30] and solid[35] states, the phenyl and vinyl groups of TMS are coplanar. It is clear that adsorbed TMS adopts a closely similar geometry, which brings the C=C bond almost parallel to the surface, thus mimicking the behavior of adsorbed propene itself.[13] Notice that in this conformation the allylic hydrogen atoms on the sp^3 carbon are in close proximity to the oxygenated surface, which should act to actually *increase* the chances of allylic hydrogen abstraction and hence combustion. The fact that appreciable epoxidation nevertheless occurs serves to underline the intrinsically high selectivity of copper. Related to this, it is interesting to note that on Ag{111} propene also adsorbs with C=C essentially parallel to the surface[36] and on Ag{110}, where it is sufficiently strongly adsorbed,[37] it undergoes only combustion.

Finally, an overall reaction scheme that is consistent with all the TPR and fast XPS data and in harmony with the NEXAFS results is shown below.

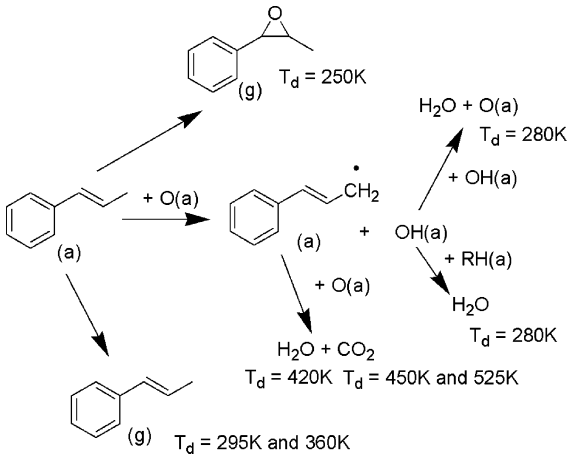

Encouraged by these results we are currently developing copper-based systems for use as practical catalysts.

Conclusions

1. Cu{111} is effective in the selective oxidation of *trans*-methylstyrene (TMS) to the epoxide, despite the presence of allylic hydrogen atoms which lie close to the oxygenated metal

(35) Cambridge Crystallographic Data Centre, database 2004.
(36) Huang, W. X.; White, J. M. *Surf. Sci.* **2002**, *513*, 399.
(37) Barteau, M. A.; Madix, R. J. *J. Am. Chem. Soc.* **1983**, *105*, 344.

surface. The behavior of the system is sensitive to the order in which reactants are adsorbed.

2. Depending on the conditions, varying amounts of oxidic oxygen are formed on the copper surface, in addition to O_a. The former leads to combustion of the alkene, and the latter induces both selective oxidation and combustion. At low temperatures, when TMS is dosed first, a metastable atomic oxygen species (O*) is formed. With increasing temperature and decreasing surface coverage, O* $\rightarrow$ O_a.

3. The O 1s XPS results and comparison with the corresponding behavior of styrene on Cu{111} strongly suggest that allylic hydrogen abstraction is indeed a critical factor that limits selectivity.

These findings suggest that the application of copper-based catalysts may provide an effective strategy for the partial oxidation of "difficult" alkenes, such as those containing labile allylic hydrogen atoms.

Acknowledgment. R.L.C. acknowledges financial support from The Cambridge University Oppenheimer fund and additional support from Johnson Matthey plc. F.J.W. acknowledges the Leverhulme Trust. The authors thank Dr S. Lizzit and Dr L. Petaccia for their assistance during the synchrotron experiments. We thank the reviewers for helpful comments and suggestions.

JA042758E